

Inhomogeneous Dust Biases Photometric Redshifts and Stellar Masses for LSST

CHANGHOON HAHN^{1,*} AND PETER MELCHIOR^{1,2}

¹*Department of Astrophysical Sciences, Princeton University, Princeton NJ 08544, USA*

²*Center for Statistics and Machine Learning, Princeton University, Princeton, NJ 08544, USA*

ABSTRACT

Spectral energy distribution (SED) modeling is one of the main methods to estimate galaxy properties, such as photometric redshifts, z , and stellar masses, M_* , for extragalactic imaging surveys. SEDs are currently modeled as light from a composite stellar population attenuated by a uniform foreground dust screen, despite evidence from simulations and observations that find large spatial variations in dust attenuation due to the detailed geometry of stars and gas within galaxies. In this work, we examine the impact of this simplistic dust assumption on inferred z and M_* for Rubin LSST. We first construct synthetic LSST-like observations (*ugrizy* magnitudes) from the NIHAO-SKIRT catalog, which provides SEDs from high resolution hydrodynamic simulations using 3D Monte Carlo radiative transfer. We then infer z and M_* from the synthetic observations using the PROVABGS Bayesian SED modeling framework. Overall, the uniform dust screen assumption biases both z and M_* in galaxies, consistently and significantly for galaxies with dust attenuation $A_V \gtrsim 0.5$, and likely below. The biases depend on the orientation in which the galaxies are observed. At $z = 0.4$, z is overestimated by ~ 0.02 for face-on galaxies and M_* is underestimated by ~ 0.4 dex for edge-on galaxies. The bias in photo- z is equivalent to the desired redshift precision level of LSST “gold sample” and will be larger at higher redshifts. Our results underscore the need for SED models with additional flexibility in the dust parameterization to mitigate significant systematic biases in cosmological analyses with LSST.

1. INTRODUCTION

The next generation of photometric galaxy surveys, e.g., the Vera C. Rubin Observatory’s Legacy Survey of Space and Time (LSST; [LSST Science Collaboration et al. 2009](#)), the ESA *Euclid* satellite mission ([Laureijs et al. 2011](#)), and the Nancy Grace Roman Space Telescope (Roman; [Spergel et al. 2015](#)), will observe billions of galaxies to probe the nature of dark matter and dark energy. Given their statistical power, cosmological analyses with these surveys will no longer be dominated by statistical uncertainties but rather by systematic biases. Systematic biases in photometric redshifts (photo- z s), in particular, will be a major limitation for these surveys as most of the primary cosmological

* changhoon.hahn@princeton.edu

analyses (weak gravitational lensing, galaxy clusters, and supernova host galaxies) rely on accurate photo- z s (Ivezić et al. 2019).

Even for current galaxy surveys, there is already evidence that systematic biases in photo- z s impact cosmological analyses. Recent weak lensing analyses of the Hyper Suprime-Cam (HSC) survey Year-3 data (Dalal et al. 2023; Li et al. 2023; More et al. 2023; Miyatake et al. 2023) account for residual systematic photo- z errors by introducing a parameter that allows the entire photo- z distribution, $n(z)$, to shift. Indeed, Miyatake et al. (2023) find that redshifts of HSC galaxies are systematically ~ 0.05 higher than the photo- z estimates. Moreover, when introducing this parameter, their S_8 constraints, a key cosmological parameter combination that measures the cosmic growth of structure, is shifted from $0.791^{+0.018}_{-0.020}$ to $0.763^{+0.040}_{-0.036}$ — a $\sim 1\sigma$ shift.

While accounting for photo- z errors by shifting the entire $n(z)$ distribution may be sufficient for current analyses, it ignores the fact that photo- z errors likely depend on galaxy properties. Hence, there is no guarantee that it will be sufficient for unbiased cosmological analyses with upcoming surveys, specifically when galaxies are grouped into various samples. Furthermore, even if it is sufficient, it roughly *halves* the constraining power of the survey.

Current methods for estimating photo- z roughly fall into two broad categories. The first are data-driven methods that bootstrap spectroscopic galaxy samples to learn the mapping between photo- z s and the more accurate and precise spectroscopic redshifts. The latest methods use self-organizing maps (e.g., Wright et al. 2020). In principle, these methods produce unbiased and robust photo- z estimates for galaxies within the selection of the spectroscopic sample. However, cosmological analyses with these methods are ultimately limited by the spectroscopic sample selection, which is almost always much shallower than photometric surveys. A large fraction of the data and constraining power from the survey hinges on a problematic calibration.

The other class of methods involve modeling of the spectral energy distribution (SED) (e.g., Brammer et al. 2008; Tanaka 2015). Going beyond fitting of spectral templates, current SED models assume that galaxy SEDs arise from composite stellar populations, which are attenuated by dust (see Conroy 2013, for a review). High-resolution galaxy formation simulations with 3D Monte Carlo dust radiative transfer (RT) reveal that variations in the “star-dust geometry”, the spatial distribution between stars and the dusty interstellar medium (ISM) produce significant spatial variation in dust attenuation (Narayanan et al. 2018). Observations have corroborated this for decades with the diversity of measured attenuation curves (e.g., Cardelli et al. 1989; Pei 1992; Calzetti et al. 2000; Conroy et al. 2010; Chevillard et al. 2013; Reddy et al. 2015). Even by eye, one easily finds dust lanes and other complex star-dust geometry within galaxies in high-resolution images. Yet most state-of-the-art models assume a simple dust geometry: a uniform foreground dust screen (e.g., da Cunha & Charlot 2011; Boquien et al. 2019; Johnson et al. 2021; Hahn et al. 2023).

In this work, we examine whether this simplistic dust assumption biases inferred photo- z s in upcoming cosmological galaxy surveys. We also consider stellar masses, M_* , another key galaxy property for cosmological analyses used to characterize how galaxy samples trace the underlying matter distribution. We focus on LSST and construct synthetic LSST-like observations from the NIHAO-SKIRT (Faucher et al. 2023), a catalog of SEDs constructed from 65 galaxies in a hydrodynamically

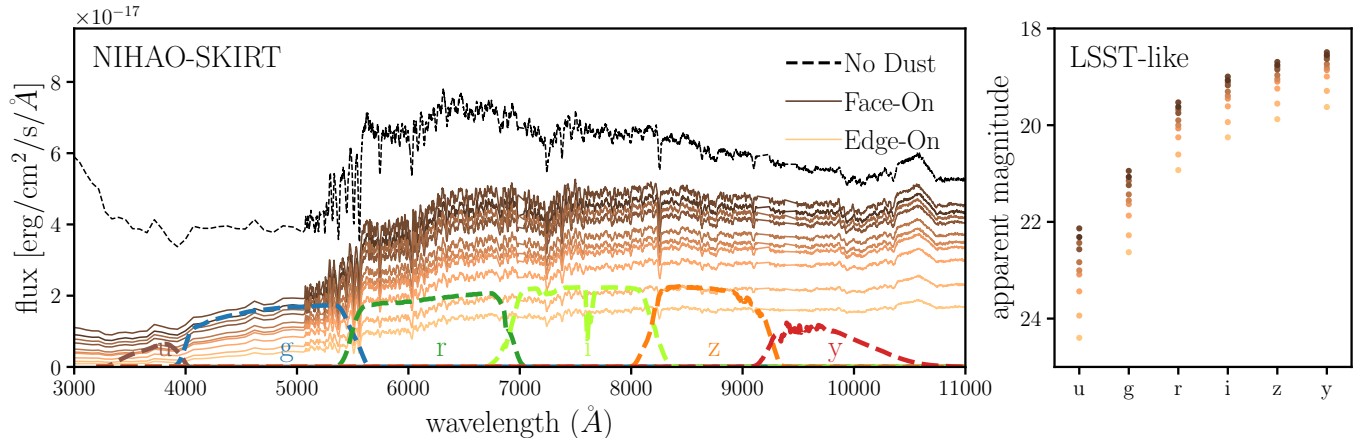


Figure 1. *Left panel:* SEDs from the NIHAO-SKIRT catalog for one of the simulated galaxies. We include the SEDs of the galaxy observed from 10 different orientations ranging from face-on to edge-on (color gradient). We also include an SED excluding dust (black dashed). The SEDs are modeled at $z = 0.4$ and their emission lines are masked. For reference, we plot the LSST broadband throughput curves (dotted). *Right panel:* Synthetic LSST magnitudes constructed from the NIHAO-SKIRT SEDs observed from the 10 different orientations. The magnitudes include LSST-like observational uncertainties.

cal simulation using stellar population synthesis (SPS) and 3D Monte Carlo RT. Then, we apply a state-of-the-art SED modeling (PROVABGS; Hahn et al. 2023) to infer z and M_* and quantify their biases.

We begin in Section 2 with a brief explanation of our synthetic LSST photometry. We then describe the SED modeling framework used to infer photo- z and M_* in Section 3. Afterwards, we present the results and discuss their implications in Section 4.

2. NIHAO-SKIRT CATALOG

We construct our synthetic LSST observations using the NIHAO-SKIRT catalog (Faucher et al. 2023). NIHAO-SKIRT provides the SEDs of 65 galaxies from the Numerical Investigation of Hundred Astrophysical Objects (NIHAO) hydrodynamical simulation suite (Wang et al. 2015). The SEDs are constructed using stellar population synthesis (SPS) with FSPS (Conroy et al. 2009; Conroy & Gunn 2010; Johnson et al. 2023) and 3D Monte Carlo radiative transfer using SKIRT (Camps & Baes 2020). The SPS assumes a Chabrier (2003) stellar initial mass function and uses the MIST isochrones (Paxton et al. 2011, 2013, 2015; Choi et al. 2016; Dotter 2016) and the MILES spectral library (Sánchez-Blázquez et al. 2006). The dust attenuation and emission from diffuse interstellar medium (ISM) is then calculated with SKIRT, which uses the THEMIS dust modeling framework (Jones et al. 2017). For young stellar populations, Faucher et al. (2023) uses a subgrid recipe because photodissociation regions are unresolved in the NIHAO galaxies. NIHAO-SKIRT is based on multiphase ISM and, thus, has more realistic dust density structure and diverse attenuation curves in comparison to previous works by, e.g., Hayward & Smith (2015); Lower et al. (2020); Trčka et al. (2020). In total, the NIHAO-SKIRT catalog provide 650 SEDs of 65 NIAHO galaxies each observed from 10 different

orientations that range from roughly face-on to roughly edge-on. It also includes matching SEDs that exclude any effect of dust.

We construct our synthetic LSST observations from the NIHAO-SKIRT SEDs, which are modeled at a distance of 100 Mpc. First, we “dry-redshift” the SEDs to $z = 0.4$ — i.e., we redshift the wavelength of the SED and scale fluxes by the new luminosity distance. We then mask emission line of the SEDs and convolve them with the LSST photometric broadband filters in the *ugrizy*-bands. We mask the emission lines to mitigate any model misspecifications: SPS does not include the contributions from nebular gas and the PROVABGS SED model does not model emission lines. Lastly, we incorporate realistic LSST-like observational uncertainties to the modeled photometric magnitudes. We apply Gaussian noise with a magnitude-dependent amplitude. More specifically, we use the magnitude error versus apparent magnitude relation in [Graham et al. \(2018\)](#), which is constructed using the [Connolly et al. \(2014\)](#) LSST simulation package.

In Figure 1, we present the NIHAO-SKIRT SEDs (left panel) and the synthetic LSST magnitudes constructed from them (right panel) for a single simulated NIHAO galaxy. In the left panel, we present the SEDs of the galaxy observed from 10 different orientations. The color gradient represent the orientation ranging from edge-on to face-on: light to dark. We also include an SED excluding any effects of dust (black dashed), observed edge-on. The SEDs are modeled at $z = 0.4$ and their emission lines are masked. For reference, we plot the LSST broadband throughput curves (dotted). In the right panel, we present the synthetic LSST magnitudes for the 10 different orientations. The error bar represent the LSST-like observational uncertainties that we include; however, they are negligible in the figure.

3. SED MODELING WITH PROVABGS

We infer photo- z and M_* from the synthetic LSST magnitudes using the PROVABGS Bayesian SED modeling framework ([Hahn et al. 2023](#); [Kwon et al. 2023](#)). PROVABGS models galaxy SEDs using SPS based on FSPS with MIST isochrones, MILES stellar libraries, and the [Chabrier \(2003\)](#) IMF. These are the same modeling choices as the SPS in NIHAO-SKIRT. Furthermore, PROVABGS uses a non-parametric star-formation history (SFH) with a starburst and a non-parametric evolving metallicity history (ZH). These prescriptions are derived from SFHs and ZHs of simulated galaxies in the Illustris hydrodynamic simulation ([Vogelsberger et al. 2014](#); [Genel et al. 2014](#); [Nelson et al. 2015](#)) and provide compact and flexible representations of a wide range of SFHs and ZHs.

For dust attenuation, PROVABGS uses the two-component [Charlot & Fall \(2000\)](#) model with birth cloud and ISM components. Both components are modeled as a uniform foreground dust screen that attenuates all of the star light from a galaxy. We use PROVABGS primarily for its speed and convenience: e.g., PROVABGS enables accelerated inference through neural emulators for the SED model ([Kwon et al. 2023](#)).

For the Bayesian inference, we estimate the posteriors using the Preconditioned Monte Carlo algorithm `pocomc`¹ ([Karamanis et al. 2022a,b](#)). In total the PROVABGS SED model that we use has 13 parameters: photo- z , M_* , 6 parameters specifying the SFH ($\beta_1, \beta_2, \beta_3, \beta_4, f_{\text{burst}}, t_{\text{burst}}$), 2 parameters

¹ <https://pocomc.readthedocs.io/en/latest/>

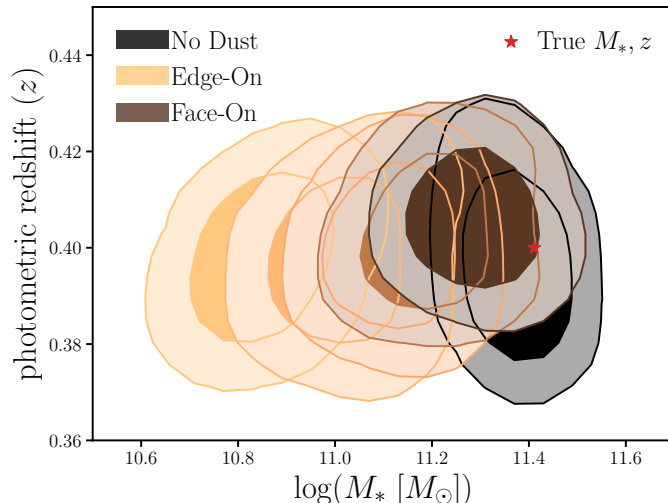


Figure 2. Posteriors, $p(z, M_* | \mathbf{X}_{i,j})$, for a single simulated NIHAO-SKIRT galaxy ($i = 64$) observed from different orientations, j . We present five of the ten orientations ranging from edge-on to face-on (light to dark). We also include the posterior inferred from $\mathbf{X}_{i,j}^{\text{no dust}}$, LSST photometry constructed from SEDs with no dust (black), as well as the true z and M_* (red star). *Dust introduces orientation dependent biases in the inferred z and M_* .*

specifying ZH (γ_1, γ_2), and 3 parameters specifying dust attenuation ($\tau_{\text{BC}}, \tau_{\text{ISM}}, n_{\text{dust}}$). PROVABGS infers full posteriors over all 13 parameters, but for this work we focus solely on the posteriors of z and M_* . To emphasize the critical point of this paper: Our SED model does include dust attenuation from birth clouds and ISM but, like other current SED models (e.g., Prospector, Johnson et al. 2021; CIGALE, Noll et al. 2009; Boquien et al. 2019), it treats dust as a homogeneous screen, whereas galaxies show highly inhomogeneous dust. We want to know how this model misspecification affects SED parameter constraints on z and M_* .

4. RESULTS & DISCUSSION

We use PROVABGS to infer the posteriors of z and M_* from the LSST-like magnitudes with and without dust, $\mathbf{X}_{i,j}^{\text{dust}}$ and $\mathbf{X}_{i,j}^{\text{no dust}}$, for $i = 1, \dots, 65$ NIHAO galaxies observed at $j = 1, \dots, 10$ orientations. In Figure 2, we present the posteriors for a single massive galaxy ($i = 64$, $M_{*,i} = 10^{11.41} M_\odot$) at different orientations ranging from edge-on to face-on (light to dark): $p(z, M_* | \mathbf{X}_{64,j}^{\text{dust}})$. We select five out of ten orientations for clarity. For reference, we include $p(z, M_* | \mathbf{X}_{64,j}^{\text{no dust}})$, the posterior inferred using the magnitudes without any dust (black). We also mark the true z and M_* of the galaxy (red).

For all galaxies, the posteriors have consistent precision on the z and M_* constraints: $\sigma_z \sim 0.01$ and $\sigma_{\log M_*} \sim 0.07$. Their accuracy, however, significantly differ. First, for photometry without dust, we are able to infer a posterior that is fully consistent with the true z and M_* . Meanwhile, the posteriors for photometry with dust shift significantly. For photo- z , the inferred z has a noticeable dependence on galaxy orientation: we infer higher z for more face-on orientations. For the most face-on orientation, the inferred z is slightly higher than the true z — though statistically consistent. For M_* , the inferred values are increasingly underestimated for more edge-on orientations. The trend is

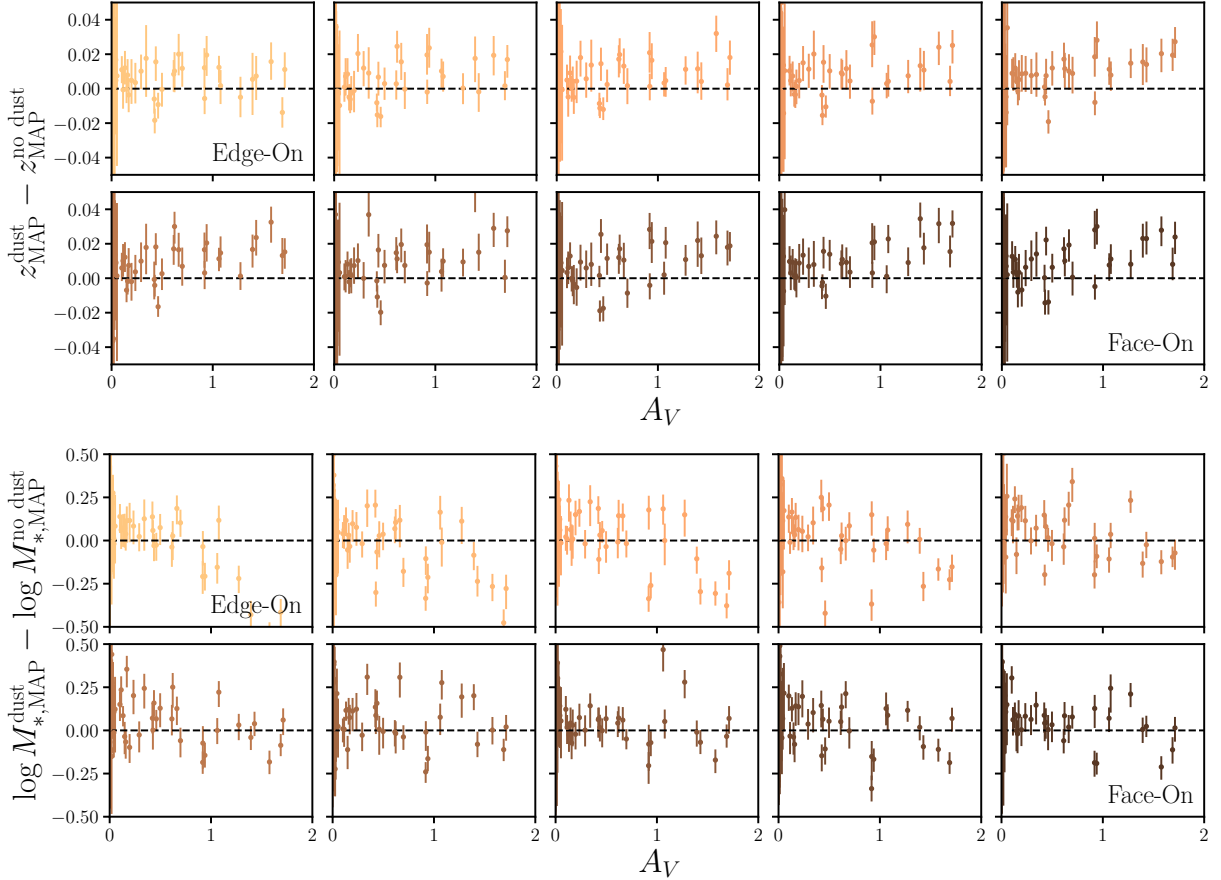


Figure 3. The effect of dust on inferred photo- z (top) and M_* (bottom). We present the difference between the MAP values of $p(z, M_* | \mathbf{X}_{i,j}^{\text{dust}})$ and $p(z, M_* | \mathbf{X}_{i,j}^{\text{no dust}})$ as a function of A_V . Each panel and color presents a different orientation from edge-on (top left; light) to face-on (bottom right; dark). With $A_V \lesssim 0.5$ we infer overall unbiased z and M_* . With $A_V > 0.5$, there is a bias in photo- z s that depends on orientation: photo- z s are overestimated for more face-on orientations. For face-on, photo- z s are overestimated by ~ 0.02 . There is also a bias in M_* that depends on orientation: M_* is underestimated for more edge-on orientations. For edge-on, M_* are underestimated by ~ 0.4 dex. The current uniform dust screen assumption in SED modeling is insufficient at marginalizing the effect of dust and will impact LSST cosmological analyses.

significant and monotonic. For the most edge-on orientation, the inferred M_* is more than 0.5 dex lower than the true value — a discrepancy of $>4\sigma$.

We examine the role of dust and galaxy orientation further, in Figure 3. We compare the posteriors from photometry with dust versus without dust for photo- z (top) and M_* (bottom) as a function of dust attenuation in the V -band, A_V . In particular, we present the differences between the maximum-a-posterior (MAP) values of $p(z, M_* | \mathbf{X}_{i,j}^{\text{dust}})$ and of $p(z, M_* | \mathbf{X}_{i,j}^{\text{no dust}})$ for all 65 NIHAO galaxies. The errorbars represent the 16 and 84th percentiles of $p(z, M_* | \mathbf{X}_{i,j}^{\text{dust}})$, for reference. Each panel and color presents the differences for a single galaxy orientation ranging from edge-on (top left; light) to face-on (bottom right; dark).

We compare $p(z, M_* | \mathbf{X}_{i,j}^{\text{dust}})$ against $p(z, M_* | \mathbf{X}_{i,j}^{\text{no dust}})$, instead of against the true z and M_* , to isolate the effects of dust from the broader model misspecification issues in SED modeling. Although we find overall good consistency between $p(z, M_* | \mathbf{X}_{i,j}^{\text{no dust}})$ and the true values, [Faucher & Blanton \(2024\)](#) recently find that model misspecification can significantly bias, e.g., inferred SFRs by more than a factor of 3. In this work, we solely focus on the impact of dust in biasing photo- z and M_* ; we refer readers to [Faucher & Blanton \(2024\)](#) for a broader examination of model misspecification in SED modeling.

For the NIHAO galaxies with higher dust attenuation ($A_V > 0.5$), [Figure 3](#) reveals a significant orientation dependent bias, consistent with [Figure 2](#). For photo- z , more face-on orientations overestimate z . photo- z s are overall unbiased for the edge-on orientation but overestimated by ~ 0.02 for the face-on orientation. This corresponds to roughly a $2\sigma_z$ bias. It is also equivalent to the desired precision level of the high signal-to-noise LSST “gold sample”, which will be used for the majority of cosmological analyses ([LSST Science Collaboration et al. 2009](#)). For lower dust attenuation ($A_V \lesssim 0.5$), the results are inconclusive given the photometric errors of individual galaxies, but are likely still biased when aggregating larger samples.

There is also an orientation dependent bias for M_* , where M_* is significantly underestimated for more edge-on orientations. The inferred M_* values are overall unbiased for the face-on orientation but underestimated by ~ 0.4 dex for the edge-on orientation. This corresponds to a $> 4\sigma_{M_*}$ bias. We note that this bias in M_* is consistent with the M_* bias found in [Faucher & Blanton \(2024\)](#) using different SED modeling methods.

The biases in z and M_* come from the fact that dust significantly impacts the photometry of galaxies, but the parameters of a SED model that best fit the attenuated photometry are inconsistent with the ones that best fit the unattenuated photometry. In other words, the dust attenuation model in our SED model does not sufficiently marginalize over the effect of dust. Hence, the assumption of a uniform dust screen is insufficient for the precision level of LSST photometry. Interestingly, we find that the uniform dust screen assumption breaks down even for face-on galaxies. Edge-on galaxies will generally have significantly more attenuation than face-on galaxies, as stellar light will need to travel through more of the dust-filled ISM. Nevertheless, photo- z s are biased for face-on galaxies.

The bias in photo- z s has significant implications for LSST cosmological analyses. As mentioned above, biases in photo- z measurements of source galaxies in weak lensing analyzes significantly bias S_8 constraints (e.g., [More et al. 2023](#)). We find significant photo- z bias for galaxies with $A_V > 0.5$. In our NIHAO sample this consists of massive galaxies with $M_* > 10^{10} M_\odot$. For LSST weak lensing galaxies, the sample will include galaxies brighter than $i < 25.3$ spanning $0.35 \lesssim z \lesssim 2$ ([LSST Science Collaboration et al. 2009](#)). Given the selection and wide redshift range, we expect that the impact of dust will be more significant than our findings at $z = 0.4$ and show a significant redshift dependence.

First, with the magnitude cut, the fraction of massive galaxies will increase with redshift. Since more massive galaxies generally have more dust (e.g., [Ciesla et al. 2014](#); [Rémy-Ruyer et al. 2014](#); [Santini et al. 2014](#)), the impact of dust in biasing photo- z s will also increase with redshift. The overall photo- z bias will also be made worse due to differences in the properties of galaxies at higher redshift. Higher redshift galaxies have higher dust fractions. For instance, [Santini et al. \(2014\)](#) find,

for a galaxy sample with FIR observations, that at fixed M_* galaxies at $z \sim 2$ have ~ 10 times higher dust fraction than galaxies at $z \sim 0.4$. Thus, we can expect dust to bias photo- z s at even lower masses at higher redshifts.

Beyond the increased bias in photo- z s, the redshift dependence of the increase implies that bias will not simply shift the overall $n(z)$. Since higher-redshift galaxies will be more biased, the bias will change the overall shape of $n(z)$. Therefore, introducing a parameter that shifts $n(z)$, as in the HSC analyses, will not fully account for this effect for LSST weak-lensing analyses.

The bias in M_* also has significant implications for LSST. M_* is a key physical property used to study galaxy evolution and measure, e.g., galaxy mass assembly. Furthermore, it plays a critical role in understanding the galaxy-halo connection through galaxy bias or abundance matching (see [Wechsler & Tinker 2018](#) for a review). For cosmological analyses, the galaxy-halo connection is a key component in construct large-volume simulations for estimating the covariance matrices of observables and validating the analyses. Since dust leads to systematic underestimates of M_* , it can lead us to mischaracterize the galaxy-halo connection.

Fortunately, it is possible to mitigate the impact of dust on the inferred photo- z s and M_* . The main issue stems from model misspecification caused by the uniform dust screen assumption in SED models. We therefore recommend the adoption of non-uniform dust screens that include multiple dust components (e.g., [Lower et al. 2022](#)), which will provide a more flexible description of a wider range of dust attenuation curves and, thus, enable us to better marginalize over the effect of dust. One consequence of this approach, or any increase in the flexibility of the model, is that the constraints on photo- z s and M_* will get weaker. In future work, we will investigate ways to determine spatial dust distributions to provide unbiased SED-derived parameters, regain some or all of the constraining power of photometric survey data, and study the relation between stellar and dust morphologies of galaxies.

ACKNOWLEDGEMENTS

It's a pleasure to thank Nicholas Faucher and Michael R. Blanton for useful discussions and for publicly releasing the NIHAO-SKIRT catalog. This work was supported by the AI Accelerator program of the Schmidt Futures Foundation. This work was substantially performed using the Princeton Research Computing resources at Princeton University, which is a consortium of groups led by the Princeton Institute for Computational Science and Engineering (PICSciE) and Office of Information Technology's Research Computing.

REFERENCES

- | | |
|--|--|
| <p>Boquien, M., Burgarella, D., Roehlly, Y., et al. 2019, <i>Astronomy and Astrophysics</i>, 622, A103, doi: 10.1051/0004-6361/201834156</p> <p>Brammer, G. B., van Dokkum, P. G., & Coppi, P. 2008, <i>ApJ</i>, 686, 1503, doi: 10.1086/591786</p> | <p>Calzetti, D., Armus, L., Bohlin, R. C., et al. 2000, <i>The Astrophysical Journal</i>, 533, 682, doi: 10.1086/308692</p> <p>Camps, P., & Baes, M. 2020, <i>Astronomy and Computing</i>, 31, 100381, doi: 10.1016/j.ascom.2020.100381</p> |
|--|--|

- Cardelli, J. A., Clayton, G. C., & Mathis, J. S. 1989, *The Astrophysical Journal*, 345, 245, doi: [10.1086/167900](https://doi.org/10.1086/167900)
- Chabrier, G. 2003, *Publications of the Astronomical Society of the Pacific*, 115, 763, doi: [10.1086/376392](https://doi.org/10.1086/376392)
- Charlot, S., & Fall, S. M. 2000, *The Astrophysical Journal*, 539, 718, doi: [10.1086/309250](https://doi.org/10.1086/309250)
- Chevallard, J., Charlot, S., Wandelt, B., & Wild, V. 2013, *Monthly Notices of the Royal Astronomical Society*, 432, 2061, doi: [10.1093/mnras/stt523](https://doi.org/10.1093/mnras/stt523)
- Choi, J., Dotter, A., Conroy, C., et al. 2016, *The Astrophysical Journal*, 823, 102, doi: [10.3847/0004-637X/823/2/102](https://doi.org/10.3847/0004-637X/823/2/102)
- Ciesla, L., Boquien, M., Boselli, A., et al. 2014, *Astronomy and Astrophysics*, 565, A128, doi: [10.1051/0004-6361/201323248](https://doi.org/10.1051/0004-6361/201323248)
- Connolly, A. J., Angeli, G. Z., Chandrasekharan, S., et al. 2014, 9150, 915014, doi: [10.1117/12.2054953](https://doi.org/10.1117/12.2054953)
- Conroy, C. 2013, *Annual Review of Astronomy and Astrophysics*, 51, 393, doi: [10.1146/annurev-astro-082812-141017](https://doi.org/10.1146/annurev-astro-082812-141017)
- Conroy, C., & Gunn, J. E. 2010, *The Astrophysical Journal*, 712, 833, doi: [10.1088/0004-637X/712/2/833](https://doi.org/10.1088/0004-637X/712/2/833)
- Conroy, C., Gunn, J. E., & White, M. 2009, *The Astrophysical Journal*, 699, 486, doi: [10.1088/0004-637X/699/1/486](https://doi.org/10.1088/0004-637X/699/1/486)
- Conroy, C., Schiminovich, D., & Blanton, M. R. 2010, *The Astrophysical Journal*, 718, 184, doi: [10.1088/0004-637X/718/1/184](https://doi.org/10.1088/0004-637X/718/1/184)
- da Cunha, E., & Charlot, S. 2011, *Astrophysics Source Code Library*, ascl:1106.010
- Dalal, R., Li, X., Nicola, A., et al. 2023, *Physical Review D*, 108, 123519, doi: [10.1103/PhysRevD.108.123519](https://doi.org/10.1103/PhysRevD.108.123519)
- Dotter, A. 2016, *The Astrophysical Journal Supplement Series*, 222, 8, doi: [10.3847/0067-0049/222/1/8](https://doi.org/10.3847/0067-0049/222/1/8)
- Faucher, N., & Blanton, M. R. 2024, *Testing the Accuracy of SED Modeling Techniques Using the NIHAO-SKIRT-Catalog*, doi: [10.48550/arXiv.2404.19742](https://doi.org/10.48550/arXiv.2404.19742)
- Faucher, N., Blanton, M. R., & Macciò, A. V. 2023, *ApJ*, 957, 7, doi: [10.3847/1538-4357/acf9f0](https://doi.org/10.3847/1538-4357/acf9f0)
- Genel, S., Vogelsberger, M., Springel, V., et al. 2014, *Monthly Notices of the Royal Astronomical Society*, 445, 175, doi: [10.1093/mnras/stu1654](https://doi.org/10.1093/mnras/stu1654)
- Graham, M. L., Connolly, A. J., Ivezić, Ž., et al. 2018, *The Astronomical Journal*, 155, 1, doi: [10.3847/1538-3881/aa99d4](https://doi.org/10.3847/1538-3881/aa99d4)
- Hahn, C., Kwon, K. J., Tojeiro, R., et al. 2023, *ApJ*, 945, 16, doi: [10.3847/1538-4357/ac8983](https://doi.org/10.3847/1538-4357/ac8983)
- Hayward, C. C., & Smith, D. J. B. 2015, *Monthly Notices of the Royal Astronomical Society*, 446, 1512, doi: [10.1093/mnras/stu2195](https://doi.org/10.1093/mnras/stu2195)
- Ivezić, Ž., Kahn, S. M., Tyson, J. A., et al. 2019, *The Astrophysical Journal*, 873, 111, doi: [10.3847/1538-4357/ab042c](https://doi.org/10.3847/1538-4357/ab042c)
- Johnson, B., Foreman-Mackey, D., Sick, J., et al. 2023, *dfm/python-fsps: v0.4.6, v0.4.6*, Zenodo, doi: [10.5281/zenodo.10026684](https://doi.org/10.5281/zenodo.10026684)
- Johnson, B. D., Leja, J., Conroy, C., & Speagle, J. S. 2021, *ApJS*, 254, 22, doi: [10.3847/1538-4365/abef67](https://doi.org/10.3847/1538-4365/abef67)
- Jones, A. P., Köhler, M., Ysard, N., Bocchio, M., & Verstraete, L. 2017, *Astronomy and Astrophysics*, 602, A46, doi: [10.1051/0004-6361/201630225](https://doi.org/10.1051/0004-6361/201630225)
- Karamanis, M., Beutler, F., Peacock, J. A., Nabergoj, D., & Seljak, U. 2022a, *Monthly Notices of the Royal Astronomical Society*, 516, 1644
- Karamanis, M., Nabergoj, D., Beutler, F., Peacock, J. A., & Seljak, U. 2022b, *arXiv preprint arXiv:2207.05660*
- Kwon, K. J., Hahn, C., & Alsing, J. 2023, *The Astrophysical Journal Supplement Series*, 265, 23, doi: [10.3847/1538-4365/acba14](https://doi.org/10.3847/1538-4365/acba14)
- Laureijs, R., Amiaux, J., Arduini, S., et al. 2011, *arXiv e-prints*, arXiv:1110.3193
- Li, X., Zhang, T., Sugiyama, S., et al. 2023, *Physical Review D*, 108, 123518, doi: [10.1103/PhysRevD.108.123518](https://doi.org/10.1103/PhysRevD.108.123518)
- Lower, S., Narayanan, D., Leja, J., et al. 2020, *The Astrophysical Journal*, 904, 33, doi: [10.3847/1538-4357/abbfa7](https://doi.org/10.3847/1538-4357/abbfa7)
- . 2022, *The Astrophysical Journal*, 931, 14, doi: [10.3847/1538-4357/ac6959](https://doi.org/10.3847/1538-4357/ac6959)
- LSST Science Collaboration, Abell, P. A., Allison, J., et al. 2009, *arXiv:0912.0201 [astro-ph]*, <https://arxiv.org/abs/0912.0201>

- Miyatake, H., Sugiyama, S., Takada, M., et al. 2023, *Physical Review D*, 108, 123517, doi: [10.1103/PhysRevD.108.123517](https://doi.org/10.1103/PhysRevD.108.123517)
- More, S., Sugiyama, S., Miyatake, H., et al. 2023, *Physical Review D*, 108, 123520, doi: [10.1103/PhysRevD.108.123520](https://doi.org/10.1103/PhysRevD.108.123520)
- Narayanan, D., Conroy, C., Davé, R., Johnson, B. D., & Popping, G. 2018, *The Astrophysical Journal*, 869, 70, doi: [10.3847/1538-4357/aaed25](https://doi.org/10.3847/1538-4357/aaed25)
- Nelson, D., Pillepich, A., Genel, S., et al. 2015, *Astronomy and Computing*, 13, 12, doi: [10.1016/j.ascom.2015.09.003](https://doi.org/10.1016/j.ascom.2015.09.003)
- Noll, S., Burgarella, D., Giovannoli, E., et al. 2009, *Astronomy and Astrophysics*, 507, 1793, doi: [10.1051/0004-6361/200912497](https://doi.org/10.1051/0004-6361/200912497)
- Paxton, B., Bildsten, L., Dotter, A., et al. 2011, *The Astrophysical Journal Supplement Series*, 192, 3, doi: [10.1088/0067-0049/192/1/3](https://doi.org/10.1088/0067-0049/192/1/3)
- Paxton, B., Cantiello, M., Arras, P., et al. 2013, *The Astrophysical Journal Supplement Series*, 208, 4, doi: [10.1088/0067-0049/208/1/4](https://doi.org/10.1088/0067-0049/208/1/4)
- Paxton, B., Marchant, P., Schwab, J., et al. 2015, *The Astrophysical Journal Supplement Series*, 220, 15, doi: [10.1088/0067-0049/220/1/15](https://doi.org/10.1088/0067-0049/220/1/15)
- Pei, Y. C. 1992, *The Astrophysical Journal*, 395, 130, doi: [10.1086/171637](https://doi.org/10.1086/171637)
- Reddy, N. A., Kriek, M., Shapley, A. E., et al. 2015, *The Astrophysical Journal*, 806, 259, doi: [10.1088/0004-637X/806/2/259](https://doi.org/10.1088/0004-637X/806/2/259)
- Rémy-Ruyer, A., Madden, S. C., Galliano, F., et al. 2014, *Astronomy and Astrophysics*, 563, A31, doi: [10.1051/0004-6361/201322803](https://doi.org/10.1051/0004-6361/201322803)
- Sánchez-Blázquez, P., Peletier, R. F., Jiménez-Vicente, J., et al. 2006, *Monthly Notices of the Royal Astronomical Society*, 371, 703, doi: [10.1111/j.1365-2966.2006.10699.x](https://doi.org/10.1111/j.1365-2966.2006.10699.x)
- Santini, P., Maiolino, R., Magnelli, B., et al. 2014, *Astronomy and Astrophysics*, 562, A30, doi: [10.1051/0004-6361/201322835](https://doi.org/10.1051/0004-6361/201322835)
- Spergel, D., Gehrels, N., Baltay, C., et al. 2015, *Wide-Field Infrared Survey Telescope-Astrophysics Focused Telescope Assets WFIRST-AFTA 2015 Report*
- Tanaka, M. 2015, *The Astrophysical Journal*, 801, 20, doi: [10.1088/0004-637X/801/1/20](https://doi.org/10.1088/0004-637X/801/1/20)
- Trčka, A., Baes, M., Camps, P., et al. 2020, arXiv:2003.12576 [astro-ph]. <https://arxiv.org/abs/2003.12576>
- Vogelsberger, M., Genel, S., Springel, V., et al. 2014, *Monthly Notices of the Royal Astronomical Society*, 444, 1518, doi: [10.1093/mnras/stu1536](https://doi.org/10.1093/mnras/stu1536)
- Wang, L., Dutton, A. A., Stinson, G. S., et al. 2015, *Monthly Notices of the Royal Astronomical Society*, 454, 83, doi: [10.1093/mnras/stv1937](https://doi.org/10.1093/mnras/stv1937)
- Wechsler, R. H., & Tinker, J. L. 2018, ArXiv e-prints, 1804, arXiv:1804.03097
- Wright, A. H., Hildebrandt, H., van den Busch, J. L., & Heymans, C. 2020, *A&A*, 637, A100, doi: [10.1051/0004-6361/201936782](https://doi.org/10.1051/0004-6361/201936782)